Thermodynamic Processes in the Moist Atmosphere

Banner cloud at a mountain in the Alps.
PHOTOGRAPH BIRGIT BOTT

Andreas Bott*

1811-5209/10/0006-0293$2.50 DOI: 10.2113/gselements.6.5.293

Thermodynamic principles play a key role in almost all processes occurring in the Earth's atmosphere. They are formidably expressed in the thermal stratification of the atmosphere, in the appearance of various regional and large-scale wind systems, as well as in the formation of clouds and precipitation. It is important to note that the application of simplified thermodynamics is usually sufficient to describe large-scale atmospheric processes. However, for an in-depth understanding of the microphysical structure of clouds, a detailed investigation of the complex thermodynamic cloud processes is needed.

KEYWORDS: adiabatic process, cloud microphysics, phase diagram of water, thermodynamic diagram, tropical cyclone

FUNDAMENTAL PRINCIPLES IN ATMOSPHERIC THERMODYNAMICS

In order to describe the thermodynamic state of the atmosphere and its future development, it is necessary to formulate prognostic equations for the atmospheric wind field, the air temperature, the air pressure, and the masses of dry air, water vapor, liquid water, and ice. These equations are derived on the basis of several fundamental physical principles and axioms. Newton's axioms lead to the prognostic equation for the atmospheric wind field, known as the Navier-Stokes equation. For the different masses, prognostic equations are formulated based on the principle of mass conservation. Prognostic equations for the internal energy or the enthalpy, as obtained from the first law of thermodynamics, may be used for the calculation of time rate changes of the temperature. Details about the derivation of the atmospheric thermohydrodynamic equation system may be found in standard textbooks on dynamics and thermodynamics (e.g. Bohren and Albrecht 1998; Zdunkowski and Bott 2003, 2004; North and Erukhimova 2009).

For the air pressure, p, a diagnostic relation may be obtained from the ideal gas law for moist air, yielding

$$p = \rho(m_d R_d + m_v R_v)T = \rho R_d T_v \ , \qquad (1)$$

where ρ is the air density, m_d, m_v and R_d, R_v are the mass concentrations and gas constants of dry air and water vapor, respectively, and T is the air temperature. Equation (1) is also the defining relation for the virtual temperature, T_v, which is commonly used in atmospheric thermodynamics. This quantity is the temperature of dry air having the same pressure and specific volume as the moist air. It is noteworthy that in Equation (1) the specific volumes of water and ice particles have been ignored. Under typical atmospheric conditions this assumption is certainly justified. Moreover, dry air is assumed to be an ideal gas. This treatment is based on the assumption that dry air consists of a constant mixture of ideal gases, i.e. nitrogen, oxygen, argon, carbon dioxide, and other trace gases. For atmospheric considerations, the spatiotemporal variation of the composition of dry air may safely be neglected.

THE THERMODYNAMICALLY FILTERED SYSTEM

In classical atmospheric thermodynamics it is assumed that the atmosphere is either subsaturated, yielding relative humidities, r_h, below 100%, or saturated, that is, r_h = 100%. Saturation occurs if the water vapor is in chemical equilibrium with a plane water or ice surface. According to Gibbs' phase rule, two phases of water may coexist in chemical equilibrium at different sets of temperature and pressure. Moreover, the three phases of water can occur simultaneously only at one temperature and pressure, the so-called triple point. The well-known Clausius-Clapeyron equations describe the phase diagram of water, i.e. curves of saturation vapor pressure, e_{sat}, along which two different water phases coexist in chemical equilibrium.

FIGURE 1 shows qualitatively the phase diagram of water, in which the gas, liquid, and solid phases are separated by saturation vapor pressure curves. The abscissa denotes the temperature, T, and the ordinate shows the partial pressure of water vapor, e, which is simply called *vapor pressure*. The magenta arrows indicate direct transitions between the gas and solid phases, the black arrows denote condensation/evaporation, and the yellow arrows describe the freezing and melting of water and ice. At the critical point, the physical properties of the liquid and gas phases of water become identical. At temperatures higher than the critical temperature, it is no longer possible to convert the gas phase to the liquid phase by increasing the pressure, and one speaks of a supercritical fluid.

During a thermodynamic process, a system proceeds from an initial to a final thermodynamic state, thereby changing the values of its thermodynamic state variables. The thermodynamic process is called *adiabatic* if the system is insulated. In this case there will be no heat transfer between the system and its surroundings. If in addition the entropy of the system remains constant, then the thermodynamic

* Meteorological Institute, University of Bonn
Auf dem Hügel 20, 53121 Bonn, Germany
E-mail: a.bott@uni-bonn.de

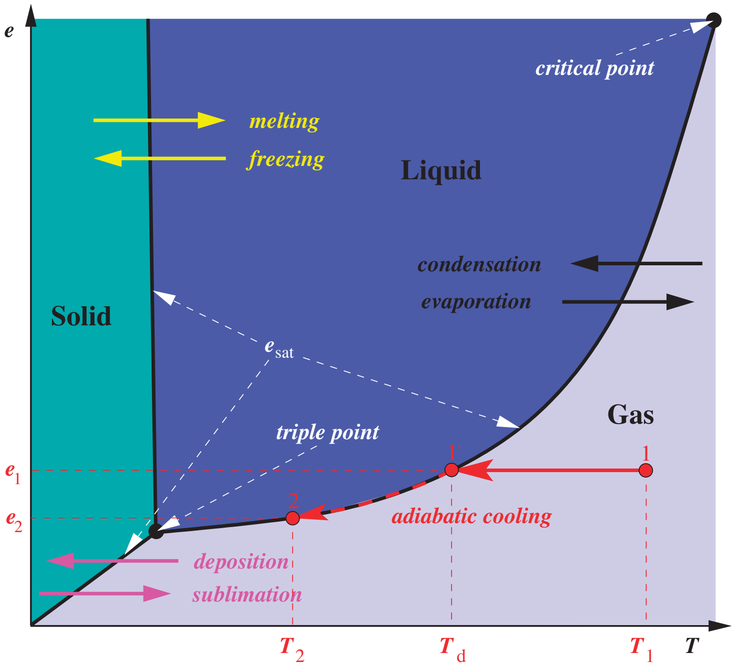

FIGURE 1 Phase diagram of water. T = air temperature; T_d = dew point temperature; e = vapor pressure; e_{sat} = saturation vapor pressure. See text for further details.

process is reversible and we speak of an isentropic process. Although, strictly speaking, there is a difference between isentropic and adiabatic processes, it is common practice to describe either process as adiabatic.

Consider the adiabatic vertical displacement of an air parcel consisting of dry air and water vapor. The displacement occurs in such a way that the air parcel remains subsaturated. Integration of the first law of thermodynamics in enthalpy form from p to p_0 = 1000 hPa shows that during the vertical lifting process the potential temperature, θ, of the air parcel remains constant. θ is defined by

$$\theta = T(p_0/p)^k \ , \quad \text{with } p_0 = 1000 \text{ hPa} \ , \tag{2}$$

where T is the temperature of the air parcel. The term k is called the exponent of the adiabat. To a very good approximation, during the vertical displacement in subsaturated air the water vapor content of the air parcel may be ignored, so that k can be approximated by the corresponding exponent of the adiabat for dry air; thus, $k \approx k_d = R_d/C_{p,d}$, where $C_{p,d}$ is the specific heat capacity of dry air at constant pressure (given in J kg^{-1} K^{-1}). By assuming that the atmosphere is in hydrostatic equilibrium, it turns out that during the adiabatic lifting process the temperature of the air parcel decreases at a rate of nearly 1 °C per 100 meters, which is called the *dry adiabatic lapse rate*.

When an air parcel with temperature T_1 and vapor pressure e_1 is dry adiabatically cooled, e.g. by vertical lifting, after some time the parcel reaches its dew point temperature, T_d. At this temperature its vapor pressure (which remains constant during the dry adiabatic cooling) equals the saturation vapor pressure, e_{sat}. In FIGURE 1 the dry adiabatic cooling process is schematically indicated by the solid red arrow between the points 1 and 1′. Further cooling of the air parcel results in the formation of liquid water (or ice). Assuming at all times chemical equilibrium of the water phases, during the moist adiabatic cooling process, the air parcel moves from point 1′ along the saturation pressure curve to point 2; see the dashed red arrow in FIGURE 1.

The amount of condensed water at point 2 is given as a function of the difference of the saturation vapor pressures, $e_1 - e_2$.

The transition of water from the gas phase to the liquid or solid phase is accompanied by the release of latent heat. Hence, the resulting adiabatic lapse rate is smaller for moist than for dry conditions. From the first law of thermodynamics, it follows that during the moist adiabatic process the so-called equivalent potential temperature, θ_e, of the air parcel remains constant. θ_e is obtained in the following way. First, the air parcel is vertically lifted until all its water vapor has condensed. Then it is brought down dry adiabatically to the pressure level p_0. Here the temperature of the air parcel is the same as its equivalent potential temperature. A very good approximation to θ_e is given by the liquid water potential temperature, θ_l, introduced by Betts (1973):

$$\theta_e \approx \theta_l = \theta \exp\left(l_v\, r_{v,sat}/C_{p,d}T\right) \ , \tag{3}$$

where l_v is the latent heat of vaporization and $r_{v,sat}$ is the saturation mixing ratio of water vapor. From this equation it may be seen that with decreasing saturation mixing ratio, θ_l reaches asymptotically the value of the potential temperature, θ.

EXAMPLES OF ATMOSPHERIC ADIABATIC PROCESSES

To describe many atmospheric processes it is often helpful to assume that they proceed adiabatically. Some examples will now be given. Turbulent mixing in the lowest part of the atmosphere, the so-called atmospheric boundary layer (ABL), produces a constant vertical distribution of the potential temperature, so that in the well-mixed subsaturated ABL the vertical temperature decrease is given by the dry adiabatic lapse rate. In synoptic meteorology, which deals with the analysis and forecasting of large-scale atmospheric processes, this fact may be used to obtain a good estimate of the temperature at the Earth's surface. For this, the temperature distribution at the pressure level of 850 hPa, as predicted by a numerical weather-prediction model, is extrapolated to the ground by assuming dry adiabatic conditions below this level. However, this rule of thumb is successful only if the mixed ABL exceeds the 850 hPa level and is subsaturated, e.g. during the summer months.

In many regions the local weather is often affected by the occurrence of katabatic winds, which are usually rather cold and dry. These orographic wind systems are caused by gravitationally driven downhill flow of high-density air that has been radiatively cooled at higher elevations. Prominent examples are the drainage winds blowing from the ice sheets in Antarctica and Greenland. The Mistral is a katabatic wind frequently observed in Provence, France, while the Bora is a well-known fall wind in the Adriatic region. In Southern California the Santa Ana winds are northeasterly, offshore winds that originate in the Great Basin. The combination of strong gravitational forces acting on the cold air and funnel effects caused by the orographic structure of the particular region can result in very high and violent wind speeds, which may even reach hurricane force. Numerical simulations have revealed that the downslope wind velocities depend on the buoyancy deficit of the current and on the length and angle of the slope (see, for example, Princevac et al. 2008). During its downhill flow the air is dry adiabatically warmed. Usually this warming does not completely offset the previous strong radiative cooling of the air at higher elevations, so that the drainage winds remain rather cold. In some situations, however, adiabatic warming may be so strong that at lower elevations the katabatic wind appears as a vigorous flow of warm or even hot air. For instance, the Santa Ana winds may lead to extremely hot and dry weather situations.

In addition to the dry adiabatic warming of the descending air, the release of latent heat sometimes becomes an important factor characterizing local wind systems. Foehn winds are observed in mountain regions all over the world; examples are the Föhn in the northern Alps, the Chinook east of the Rocky Mountains, the Halny in eastern Europe, the Bergwind in South Africa, and many others. Foehn winds occur when air is adiabatically lifted on the windward side of a mountain range and descends dry adiabatically on the lee side. If condensation takes place during the lifting process, then latent heat will be released, causing moist adiabatic cooling of the ascending air. On the lee side of the mountain, however, the descending air is dry adiabatically warmed and thus becomes much warmer than it was at the same elevation on the windward side.

CLOUDS AND PRECIPITATION

Clouds and precipitation are not only of utmost importance for life on Earth, they also undoubtedly represent the most impressive and complex phenomena of atmospheric thermodynamics. Of particular importance for the formation of clouds and precipitation is the thermal stratification of the atmosphere. In order to obtain and use this information, it is helpful to plot the vertical profiles of temperature, T, and dew point, T_d, in so-called thermodynamic diagrams. Figure 2, an example of the various forms of thermodynamic diagrams, depicts a so-called skew-T–log p diagram. The diagram consists of isotherms, isobars, dry and moist adiabats, and lines of constant saturation mixing ratios. The thick black curves denote the observed vertical temperature (T; solid line) and dew point (T_d; dashed line) profiles of the atmosphere.

Consider now an air parcel that is adiabatically lifted from the ground. In the diagram the change of the temperature, T_p, of the parcel, caused by the lifting process, is represented by the blue curve. As long as the air parcel remains subsaturated, its temperature will follow a dry adiabat on the diagram. At the so-called lifting condensation level (LCL), the parcel will be saturated. The LCL is given by the intersection of the temperature curve, T_p, with the saturation mixing ratio line that corresponds to the dew point at the ground. Further lifting of the air parcel causes moist adiabatic cooling so that above the LCL the T_p curve follows a moist adiabat. At the level of free convection (LFC), the air parcel becomes warmer than the environment. Hence, above this level the air parcel will be vertically accelerated due to its positive buoyancy. Above the equilibrium level (EL), the air parcel will again be colder than the environment, thus decelerating its vertical movement.

The formation and intensity of convective cloud cells depends on the height to which the air parcel can ascend. This height is mainly controlled by the blue and the pink areas in the figure, which are obtained from the intersection points of the T_p and T curves. The blue area describes the energy that has to be applied in order to lift the air parcel from the ground to its LFC. This energy, which is also called *convective inhibition* (CIN), may be supplied to the air parcel by dynamic processes such as turbulent mixing, the flow of the parcel over a mountain, etc. The smaller the CIN the easier it is for the air parcel to reach its LFC. The pink area describes the so-called convective available potential energy (CAPE). This energy mainly stems from the release of latent heat during the moist adiabatic ascent of the air parcel. CAPE will be converted into kinetic energy of vertical motion of the rising air. The larger the CAPE the higher and faster the air parcel will ascend in the atmosphere. Updraft velocities of more than 20 m s^{-1} may be reached (Heymsfield et al. 2009).

If the CAPE is large enough, the vertically lifted air forms a deep cumulus cloud called cumulus congestus. At still higher altitudes the cloud water starts to freeze. The freezing process is accompanied by the release of latent heat of fusion. Thus, the rising air attains even more buoyancy so that the height of the cloud increases further. In Figure 2, this is schematically shown by the magenta curve and the corresponding magenta area denoting the additional CAPE as obtained by the freezing process. As long as the EL of the liquid-water cloud is at a lower altitude than the 400 hPa level, a relatively small amount of additional CAPE by freezing might be sufficient to yield a drastic increase of the cloud-top pressure from EL to the new equilibrium level, EL′, at about 300 hPa. At this point a cumulonimbus capillatus forms (the latin word *capillatus* means “hairy”). This thunderstorm cloud is characterized by a fibrous structure in its upper region, illustrating that here the cloud consists of ice particles. If the cumulonimbus reaches very high altitudes, strong winds cause a horizontal flattening of the cloud, producing an anvil structure. This cloud type is called *cumulonimbus capillatus incus* (*incus* is the latin word for “anvil”). Figure 3 depicts a mesoscale convective systems (MCS) observed on a summer day over Sardinia. The system consists of several cumulus clouds at different stages of their lifetime. At the front of the MCS a well-developed cumulus congestus is seen, while at high altitudes a large cumulonimbus with an anvil structure has formed. This convective system produced severe rainfall, hail, and flooding.

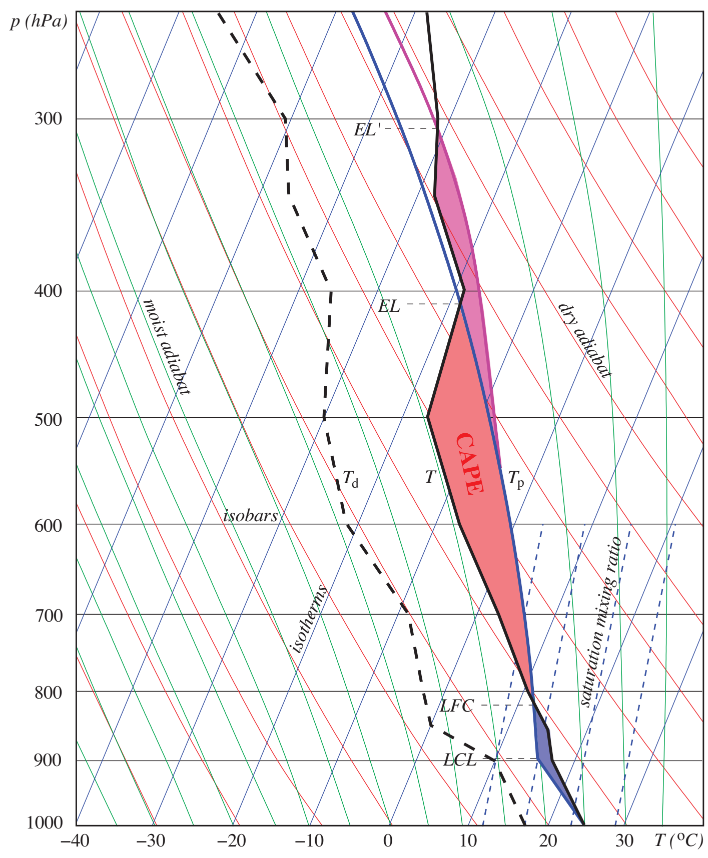

Figure 2 Skew-T versus log p diagram with vertical soundings of temperature, T, and dew point, T_d. 1000 hPa corresponds to ground level. See text for explanations.

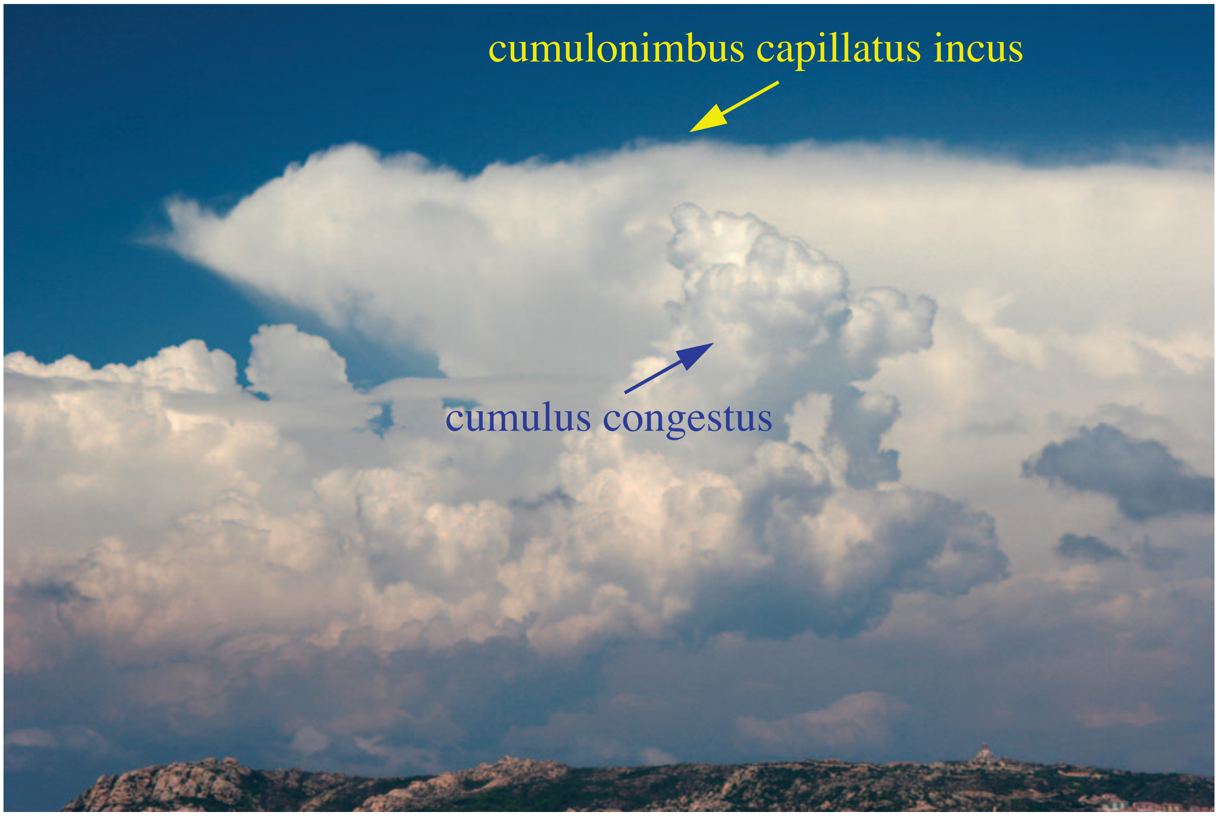

Figure 3 A mesoscale convective system over Sardinia with cumulus congestus (nearer observer) and anvil-shaped cumulus capillatus incus. This thunderstorm produced severe rainfall, hail, and flooding. Photograph: Andreas Bott

The life cycle of a thunderstorm can be subdivided into three stages. The cumulus stage is characterized by the upward motion of warm and moist air, forming a cumulus congestus. At this stage precipitation is not yet observed on the ground. In the mature stage the air reaches the equilibrium level, where it spreads out horizontally and forms a cumulonimbus capillatus. In addition to the updraft region, a small downdraft region forms within the cloud. Downdrafts are initiated by falling precipitation. Sinking air in the downdraft region is mixed with subsaturated air of the environment, so that the precipitation starts to evaporate. The associated cooling of the downdraft air by latent heat effects is very strong, thus increasing the negative buoyancy of the sinking air (Didlake and Houze 2009). This might result in very strong downbursts, sometimes exceeding 30 m s^{-1}. The strength of the vertical winds within the cloud depends mainly on the CAPE and on the vertical shear of the horizontal wind (Kirkpatrick et al. 2009). Finally, in the dissipation stage, the downdraft reaches the ground where it spreads out horizontally. The cool downdraft air cuts off the supply of warm moist air in the updraft region, so the thunderstorm starts to dissipate.

Single-cell thunderstorms form in unstable atmospheric situations, for example, during the summer or after the passage of a cold front associated with the intrusion of cold air in the upper troposphere. These so-called air-mass thunderstorms are usually not very intense. However, severe thunderstorms may evolve along strong cold fronts. In supercell thunderstorms the cloud top can reach the tropopause or even the lower stratosphere. In these storms violent tornadoes may develop. Several severe, single-cell thunderstorms are often organized into multicell clusters. These clusters can evolve into MCS, such as squall lines, mesoscale convective complexes (MCC), and tropical cyclones. While single-cell thunderstorms have a typical lifetime of less than one hour and a horizontal extent of several kilometers, an MCC is defined as a system having a cloud-top area of at least 100,000 km^2 with temperatures below –32 °C and a cloud-top area of at least 50,000 km^2 with temperatures below –52 °C. These conditions must hold for at least 6 hours.

Tropical cyclones are among the largest and most violent thermodynamic systems on Earth. The major energy source of a tropical cyclone is the release of latent heat by condensation of moisture in the rising air. This energy stems from the excessive solar energy stored in the ocean in the equatorial region. Usually water temperatures of 27 °C over a depth of 50 m are needed for the formation of a tropical cyclone. Thus, the tropical cyclone season is during the summer months (see, for example, Brennan et al. 2009; Brown et al. 2010). The most intense tropical cyclones, called typhoons or hurricanes, are characterized by a so-called eye in their center. Here, the pressure is extremely low, the winds are calm, and often no clouds exist. The eye is surrounded by the eyewall, where the most severe weather is observed. The radius of tropical cyclones may vary between less than 200 km and more than 900 km. The cover of this issue shows a satellite image of hurricane Katrina (2005), which was one of the most devastating hurricanes in the history of the United States.

In a single thunderstorm an enormous amount of water will be produced. Typical values are on the order of 10^9 kg of water. Considering that the latent heat of vaporization of water is about 2.5×10^6 J kg^{-1}, it is evident that extremely large amounts of thermal energy are released to the atmosphere during a thunderstorm. In a tropical cyclone this may result in a release of heat energy on the order of 10^{20} J per day. It is also noteworthy that the production of large amounts of cirrus anvil clouds by thunderstorms has a strong influence on the global climate (Theisen et al. 2009).

On the local scale, the vertical transport of thermal energy from the ABL into the free troposphere, due to the release of latent heat, is an important process controlling the vertical energy distribution in the atmosphere. On the global scale, the meridional transport of thermal energy in terms of latent heat plays a vital role in the maintenance of the global energy budget of Earth. This transport occurs when, in equatorial regions, a large amount of the incoming solar energy is used to evaporate water from the oceans. The water vapor is transported towards the poles where it condenses, thereby releasing the thermal energy that was needed for evaporation. The meridional transport of latent heat amounts to about 30% of the total transport of the excess thermal energy in the equatorial regions (Blüthgen and Weischet 1980). More recently, Fasullo and Trenberth (2008a, b) presented a detailed observational study of the global energy budget and its annual cycle.

CLOUD MICROPHYSICS

Atmospheric observations indicate that clouds consisting only of liquid water droplets also occur at temperatures well below 0 °C. Thus, water clouds are often supercooled. The formation of ice particles within clouds starts at a temperature of about –5 °C. The so-called mixed clouds containing water droplets and ice crystals are found at temperatures between –5 °C and –40 °C, with the fraction of ice particles increasing with decreasing temperature. Below –40 °C only pure ice clouds are generally observed.

In order to understand the thermodynamic processes occurring within clouds, a detailed investigation of cloud microstructure is necessary. The initiation of a phase change of a substance from vapor to liquid, from liquid to solid, or from vapor to solid is called nucleation. Heterogeneous nucleation takes place if other substances are involved in the phase change, whereas homogeneous nucleation describes the situation where this is not the case. As the formation of water droplets by homogeneous nucleation requires extremely high supersaturations of several hundred percent, this process is not observed in the atmosphere. On the other hand, the homogeneous nucleation of ice from supercooled water droplets is an important process controlling the formation of cirrus clouds at temperatures below –40 °C (Pruppacher and Klett 1997).

Heterogeneous nucleation of water droplets occurs on atmospheric aerosol particles (AP). These tiny particles exist everywhere in the atmosphere, but they have strongly varying number concentrations, sizes, and chemical compositions (Gieré and Querol 2010). The physicochemical characteristics of AP largely depend on how they were produced, for example, by evaporation of sea spray, wind erosion, or volcanic activity, or as emissions from terrestrial ecosystems or various anthropogenic sources, etc. AP that serve as nuclei for the formation of cloud droplets are called cloud condensation nuclei (CCN). Ice-forming nuclei (IN) are aerosol particles that are involved in the heterogeneous formation of ice particles.

A water droplet can exist over a long period of time only if it is in thermodynamic equilibrium with its environment. In this situation the vapor pressure at the droplet's surface is described by the Köhler equation which, in an approximate form, may be written as

$$e_a = e_{sat}\,(1 + A/a - B/a^3)\ . \qquad (4)$$

Here, e_a denotes the vapor pressure at the droplet's surface, a is the radius of the droplet, and A and B are functions of the physicochemical properties of the CCN. Detailed expressions for A and B may be found in standard textbooks on cloud physics (Mason 1957; Pruppacher and Klett 1997; Hobbs 2010). The term A/a yields an increase of the vapor pressure, e_a, in comparison to the saturation vapor pressure over a flat surface, e_{sat}. This term is caused by the curvature of the droplet surface and is therefore called the curvature effect. The term B/a^3, which produces a decrease of e_a compared to e_{sat}, is called the solution effect because it results from the dissolution of salts in the droplet, such as NaCl, NH_2SO_4, NH_3, and others. From Equation (4) it may be seen that for very small droplets the solution effect dominates, yielding $e_a < e_{sat}$. With increasing radius the curvature effect becomes more and more important, so that $e_a > e_{sat}$. Finally, if the droplet is large enough, $e_a \approx e_{sat}$.

Figure 4 depicts several Köhler curves describing the relationship given by Equation (4). The curves are plotted for an AP spectrum that is typical of the rural environment. With increasing relative humidity, an AP grows due to the diffusion of water vapor upon its surface. Under such conditions, the particle moves along the blue branch of its Köhler curve. As long as the supersaturation remains lower than the so-called critical supersaturation given by the red dot on the Köhler curve, the AP is in thermodynamic equilibrium. An increase of the supersaturation above the critical value brings the AP onto the green branch of its Köhler curve. Under these conditions, since e_a is lower than the supersaturation of the environment, the AP is in unstable thermodynamic equilibrium. As long as the environment remains supersaturated, an AP moving on its green curve will continue to grow by vapor diffusion. The situation where an AP enters the unstable part of its Köhler curve is called activation. All AP that have been activated form the cloud droplet spectrum.

The physicochemical properties of the AP have a strong impact on the microstructure of clouds. In regions with relatively high number concentrations of AP, at a given supersaturation a large number of AP will already be activated, resulting in a cloud with many but small droplets. In remote regions with low AP concentrations, for example,

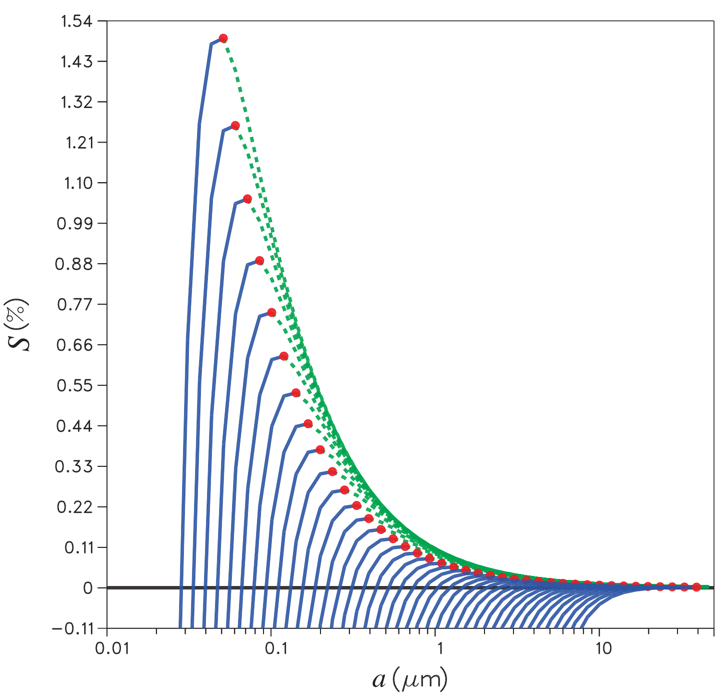

Figure 4 Köhler curves for rural aerosol particles of different sizes. a = particle radius in micrometers; $S = e_a/e_{sat} - 1$ expressed as a percent. See text for explanations.

somewhere over the ocean, at the same supersaturation only a relatively small number of AP will be activated, yielding a cloud with the same liquid water content. However, the water is partitioned onto relatively few but large droplets.

With increasing droplet size, the diffusional growth becomes more and more insufficient, finally yielding droplet radii of about 10–20 µm. The sedimentation velocity of these droplets is so small that they can barely reach the ground. For instance, a droplet of 10 µm radius needs about 14 hours to fall through a 500 m thick calm atmospheric layer, provided it does not evaporate during its descent. Considering that precipitation particles have radii exceeding 100 µm, it is obvious that additional processes are necessary to produce precipitation-sized particles. In a water cloud this occurs via the collision and coalescence of many cloud droplets. If a drop falls within the cloud it may collide and coalesce with smaller droplets having smaller fall velocities. The gravitational collisions might be enhanced by turbulent motion or by electric fields and charges of the droplets. However, the production of a single raindrop of 1 mm radius requires 10^6 cloud droplets of 10 µm radius. This is the reason why the precipitation rate is usually rather small in warm clouds. In order to obtain high precipitation rates, as for instance in thunderstorms, the ice phase must be involved.

In mixed clouds, freezing by heterogeneous nucleation is the dominant process. However, in contrast to the CCN, the IN number concentrations are usually rather small. Observations have shown that in a mixed cloud at a temperature of about –5 °C, the number concentration of ice particles might be 10^4 times larger than the IN number concentration; see, for example, Pruppacher and Klett (1997) and references therein. Several processes yield high number concentrations of ice particles in mixed clouds; such particles are referred to as secondary ice particles. The most important processes are the mechanical fracturing of fragile ice crystals, such as needles and stellar ice crystals; the shattering of large freezing drops; and the production of ice splinters during the accretion and riming of supercooled cloud droplets on ice particles, which is called the Hallet-Mossop mechanism.

Since the saturation vapor pressure with respect to ice is less than that with respect to liquid water at the same temperature, the ice particles will grow at the expense of the liquid droplets in a mixed cloud. This is called the Bergeron-Findeisen process, after T. Bergeron and W. Findeisen who developed this theory in the 1930s. Once the ice particles have gained sufficient weight, they fall out as snow. Depending on the temperature field below the cloud, melting might occur, which results in large raindrops arriving at the ground.

Consider a large cloud with high liquid water content and a higher-altitude cirrus cloud that is formed aloft by large-scale lifting processes, e.g. in orographic terrain. The ice crystals produced in the cirrus cloud may gravitationally settle down into the liquid water cloud below. Now the Bergeron-Findeisen process starts to produce a drastic increase in the precipitation rate. This phenomenon is called a seeder-feeder mechanism.

CONCLUDING REMARKS

Thermodynamic principles play a vital role in almost all atmospheric processes. They operate on spatiotemporal scales ranging from the microphysical scale of cloud droplet formation to the global scale of atmospheric motion. To a large extent, the complexity of atmospheric thermodynamics is caused by the phase transitions of water. On the microscale, the formation of liquid water droplets and ice particles is strongly affected by the physicochemical properties of the CCN and IN. Furthermore, complex interactions between the different hydrometeors occur during the generation of rain drops or snow. For large-scale investigations of atmospheric processes, it is usually sufficient to apply a simplified thermodynamic treatment by utilizing thermodynamically filtered systems. Moreover, it often seems justified to assume adiabatic motions. On the global scale, the meridional transport of energy by latent heat yields an important contribution to the Earth's energy budget. On all atmospheric scales, many important thermohydrodynamic processes are not yet fully understood. Hence, atmospheric thermodynamics will remain an interesting and challenging research field in the future.

REFERENCES

Betts AK (1973) Non-precipitating cumulus convection and its parameterization. Quarterly Journal of the Royal Meteorological Society 99: 178-196

Blüthgen J, Weischet W (1980) Allgemeine Klimageographie. De Gruyter, Berlin, New York, 887 pp

Bohren CF, Albrecht BA (1998) Atmospheric Thermodynamics. Oxford University Press, New York, 404 pp

Brennan MJ, Knabb RD, Mainelli M, Kimberlain TB (2009) Atlantic hurricane season of 2007. Monthly Weather Review 137: 4061-4088

Brown DP, Beven JL, Franklin JL, Blake ES (2010) Atlantic hurricane season of 2008. Monthly Weather Review 138: 1975-2001

Didlake AC Jr, Houze RA Jr (2009) Convective-scale downdrafts in the principal rainband of hurricane Katrina (2005). Monthly Weather Review 137: 3269-3293

Fasullo JT, Trenberth KE (2008a) The annual cycle of the energy budget. Part I: Global mean and land–ocean exchanges. Journal of Climate 21: 2297-2312

Fasullo JT, Trenberth KE (2008b) The annual cycle of the energy budget. Part II: Meridional structures and poleward transports. Journal of Climate 21: 2313-2325

Gieré R, Querol X (2010) Solid particulate matter in the atmosphere. Elements 6: 215-222

Heymsfield AJ, Bansemer A, Heymsfield G, Fierro AO (2009) Microphysics of maritime tropical convective updrafts at temperatures from –20° to –60°. Journal of the Atmospheric Sciences 66: 3530-3562

Hobbs PV (2010) Ice Physics. Oxford University Press, New York, 864 pp

Kirkpatrick C, McCaul EW Jr, Cohen C (2009) Variability of updraft and downdraft characteristics in a large parameter space study of convective storms. Monthly Weather Review 137: 1550-1561

Mason BJ (1957) The Physics of Clouds. Oxford University Press, New York, 481 pp

North GR, Erukhimova TL (2009) Atmospheric Thermodynamics. Cambridge University Press, Cambridge, 280 pp

Princevac M, Hunt JCR, Fernando HJS (2008) Quasi-steady katabatic winds on slopes in wide valleys: Hydraulic theory and observations. Journal of the Atmospheric Sciences 65: 627-643

Pruppacher HR, Klett JD (1997) Microphysics of Clouds and Precipitation. Kluwer Academic Publishers, London, 954 pp

Theisen CJ, Kucera PA, Poellot MR (2009) A study of relationships between Florida thunderstorm properties and corresponding anvil cloud characteristics. Journal of Applied Meteorology and Climatology 48: 1882-1901

Zdunkowski W, Bott A (2003) Dynamics of the Atmosphere: A Course in Theoretical Meteorology. Cambridge University Press, Cambridge, 738 pp

Zdunkowski W, Bott A (2004) Thermodynamics of the Atmosphere: A Course in Theoretical Meteorology. Cambridge University Press, Cambridge, 251 pp